Hindawi
Advances in Civil Engineering
Volume 2018, Article ID 5037057, 13 pages
https://doi.org/10.1155/2018/5037057

Research Article

Displacement Calculation Method on Front Wall of Covered Sheet-Pile Wharf

Wen-xue Gong, Li-yan Wang, Jinsong Li, and Bing-hui Wang

School of Civil and Architectural Engineering, Jiangsu University of Science and Technology, No. 2 Mengxi Road, Zhenjiang, Jiangsu Province, China

Correspondence should be addressed to Li-yan Wang; wly_yzu@163.com

Received 27 May 2018; Revised 1 November 2018; Accepted 18 November 2018; Published 24 December 2018

Academic Editor: Hugo Rodrigues

Covered sheet-pile wharves are widely used in port engineering, water conservancy, and civil engineering. This paper is based on the theory of earth pressure and the soil arching effect. According to the stress and deformation characteristics of the covered sheet-pile wharf, the formulas used to calculate the force and deformation of the front wall of a covered sheet-pile wharf under static loads are deduced. The accuracy of the theoretical derivation is verified by comparing actual measured stress and deformation data of Jingtang Port 32#. The comparison shows that when calculating the displacement of the section below the mud surface boundary, the results are in agreement with the in situ data. However, when calculating the displacement of the section above the mud surface boundary, if the anchorage point displacement is ignored because the anchorage point displacement is limited artificially, the calculated tension of the tie rod is relatively large. This leads to a significant decrease in the calculation result of the section above the mud surface boundary, which is very different from actual in situ measurement results. If anchorage point displacement is considered, the calculated tension of the tie rod is more accurate, and the calculation results of the front wall displacement are very close to in situ measurement results because the anchorage point displacement is assumed scientifically.

1. Introduction

To develop sheet-pile wharves for deep water and large berths, China Railway First Survey and Design Institute has designed and researched wharves for many years, proposed a new type of covered sheet-pile wharf in 2002, and successfully built a 100 thousand ton deep-water berth wharf [1].

Sheet-pile wharf structures include front sheet-pile walls, covered piles, anchorage walls, tie rods, and wharf equipment. The structure of a sheet-pile wharf is shown in Figure 1. It is characterized by adding a row of reinforced concrete cast-in-place piles [2], which is the covered pile, between the front walls and anchorage walls. The distance between the front sheet-pile walls is 3~5 m. Usually, covered piles are arranged in intervals. Front sheet-pile walls, covered piles, and anchorage walls are connected as a whole structure by front and rear tie rods. The existence of covered piles resists soil pressure behind the wall and reduces the soil pressure acting directly on the front sheet-pile walls. Relevant studies have shown that under normal design conditions, covered piles reduce the positive and negative bending moment of front walls by approximately 70% and 10%, respectively, and do not have a great influence on anchorage wall forces [3]. The application and development of the new type of covered sheet-pile wharf provides technical feasibility for developing sheet-pile wharves for deep water [4]. Researchers have made great efforts to research seismic analysis of anchored sheet-pile wharf walls [6–8]. Several theories and findings on the seismic analysis of sheet-pile wharves have been developed over the last several decades through experiments with shaking table tests [6, 8, 9–11]. A fundamental study on the simple evaluation method of the seismic performance of sheet-pile quay walls with vertical pile anchorage against level-one earthquake ground motion was proposed [12]. The phenomenon of the large deformation of the sheet-pile quay wall and the failure of pile foundation due to liquefaction-induced lateral spreading in a port area were investigated [13–15]. An optimization model for predicting the lateral displacement caused by liquefaction was formed by Kalantary [16]. Mitigation measures can be taken for pile groups behind quay walls subjected

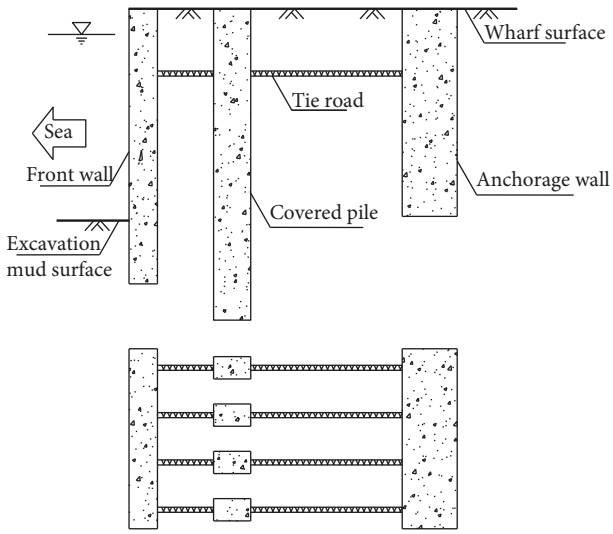

Figure 1: Diagram of blind sheet-pile wharf.

to lateral flow of liquefied soil [17]. The transfer formula for the horizontal thrust acting on the plane of covered sheet pile on land can be derived [17, 18]. Unfortunately, at present, research on covered sheet-pile wharf structures is superficial. To date, there are no systematic, reasonable, practical calculation method theories. Therefore, research on covered sheet-pile wharf structures has significant practical value.

In this paper, front wall displacement calculation was deduced theoretically based on the Winkler hypothesis. Soil pressure and displacement formulas of front sheet-pile walls in the deep part of the soil are calculated using the "m" method under static loads. Front sheet-pile walls in sheet-pile wharf forces were calculated according to the active earth pressure theory. The soil arching effect theory was combined with the lateral pressure coefficient values of parallel wall soil by doctoral student Jiang [19], and the stress on the front walls of covered sheet-pile wharves was calculated. Displacement formulas for the deformation of the front walls of a sheet-pile wharf under static load were derived based on the deflection curve equation and deformation characteristics of the material mechanics.

Finally, using a relatively mature theory of static earth pressure and soil arching effect theory, displacement formulas for the front wall of a covered sheet-pile wharf under static load are deduced and are compared with in situ observation data of the Jingtang Port 10# berth wharf and the Jingtang Port 32# wharf to verify the accuracy of the theoretical derivation.

2. Winkler's Assumption

In the elastic foundation reaction method based on Winkler's assumption, pile calculation assumes the ground reaction force p is proportional to the n-th power of the pile displacement y, that is,

$$p = K(h)y^n, \tag{1}$$

where y is the lateral deflection of the pile calculation point (m), h is the depth of the pile calculation point (m), and $K(h)$ is the ground coefficient.

Matlock and Rees [20] noted that the ground coefficient $K(h)$ should be as simple as possible, and two kinds of relations are suggested, namely,

$$K(h) = mh^q, \tag{2}$$

$$K(h) = m_0 + m_1 h + m_2 h^2. \tag{3}$$

Currently, according to some measured data and from the perspective of practicality and convenient analysis, the foundation coefficient $K(h)$ is considered to change with a power-law function with depth h consistent with the actual depth, that is,

$$K(h) = m(h_0 + h)^a, \tag{4}$$

where m is the proportional coefficient, while the foundation coefficient varies with depth, a is the pure values that change with rock type [21–24], and h_0 is a constant related to the category of rock soil. The values of m, a, and h must be determined by experiments. According to the different values of a, the law of foundation coefficient changing with depth in equation (1) can be drawn as shown in Figure 2.

3. Displacement Calculation of Front Wall

3.1. Simplified Calculation Model and Earth Pressure Area Distribution of Covered Sheet-Pile Wharf Structure. The covered sheet-pile wharf calculation model is composed of front sheet-pile walls, covered piles, anchorage walls, and front and rear tie rods, as shown in Figure 3. When calculating earth pressure, the soils are assumed to be in limit equilibrium, while the effect of wave force is not considered.

The largest difference between the covered sheet-pile wharf and the conventional sheet-pile wharf structure is that covered piles are set up between the front walls and anchorage walls, and covered piles resist the soil behind the piles and decrease the earth pressure loaded directly on the front walls. To analyse the effects of covered piles in detail, soils are divided into five regions to be discussed separately. Areas 1 and 4 are the front sheet-pile wall and covered pile, respectively, which are in soil. Since the horizontal displacement of the structure under static loads is relatively small, an elastic resistance method is adopted to calculate the horizontal earth pressure and the horizontal resistance coefficient depends on the "m" method. The earth pressure in areas 2 and 3 is more complex. Soils in these areas are between front sheet-pile walls and covered piles. The relative displacement between front sheet-pile walls and covered piles has an important influence on the amount of earth pressure. In practical engineering design, covered pile stiffness is often designed to be larger to reduce the front wall earth pressure. As a result, front-wall displacement is greater than covered-pile displacement. Soils between front walls and covered piles tend to move towards the sea, and earth pressure is partial to an active state. Therefore, earth pressure coefficients in areas 2 and 3 should be between the active earth pressure and stationary earth pressure. In this paper, Jiang Bo, a doctoral student at Zhejiang University, concluded that the lateral pressure coefficients of parallel wall

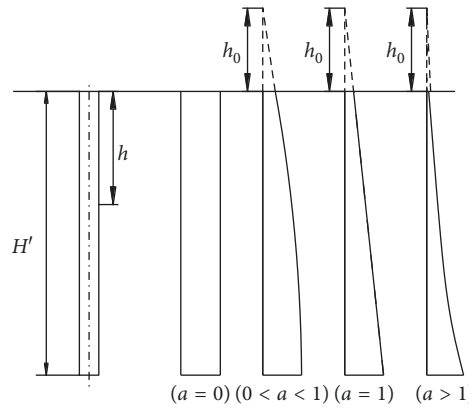

Figure 2: Law of foundation coefficient changing with depth.

soils should be used. Recommended lateral pressure coefficients are shown in Table 1.

3.2. Earth Pressure Calculation between Front Sheet-Pile Walls and Covered Piles. The lateral earth pressure between front sheet-pile walls and covered piles is usually calculated using the parallel wall theory. When calculating, a unit wall width is taken along the front sheet-pile wall width in the horizontal direction. The distance between tie rods can also be selected as a calculation unit. In the vertical direction, the microcell d_z is taken deep along the wall. Then, force analyses of the microcell are carried out. The vertical stress σ_z can be obtained using the equilibrium equation integral. The lateral earth pressure at any depth of the front sheet-pile wall can be obtained by multiplying the vertical stress σ_z by the lateral pressure coefficient K_w [25].

According to the parallel wall theory, along the length of a parallel wall cross section, at any depth z, thickness B is used in microsoil, as shown in Figure 4. The unit width is calculated to analyse the microsoil forces:

(1) Soil weight, dW:

$$dW = \gamma L \times 1 \times d_z. \tag{5}$$

(2) Upper and lower surface pressure of microsoil:
Vertical pressure of upper surface:

$$p_1 = \sigma_z \times L \times 1. \tag{6}$$

Vertical pressure of lower surface:

$$p_2 = (\sigma_z + d\sigma_z) \times L \times 1. \tag{7}$$

(3) Friction near microsoil:

$$\tau\, dz \times 1 = \sigma_x \times dz \times 1 \times \tan\delta, \tag{8}$$

$$\sigma_x = \sigma_z K_w, \tag{9}$$

where δ is the friction angle of soils near the front sheet-pile walls. The friction angle can be selected according to roughness and drainage conditions:

(1) Smooth and poorly drained, $\delta = (0 \sim (1/3))\phi$
(2) Rough and well drained, $\delta = ((1/3) \sim (1/2))\phi$
(3) Very rough and well drained, $\delta = ((1/2) \sim (2/3))\phi$

The above equilibrium equation can be obtained according to a vertical force balance of microelements:

$$\gamma L\, dz + \sigma_z L - (\sigma_z + d\sigma_z)L - 2\sigma_z K_w\, dz \tan\delta = 0, \tag{10}$$

$$\sigma_z = \frac{\gamma}{A} + Ce^{-Az}. \tag{11}$$

Boundary condition:

$$\sigma_{z=0} = q. \tag{12}$$

Taking equation (12) into account,

$$\sigma_z = \frac{1}{A}\left[\gamma - (\gamma - Aq)e^{-Az}\right]. \tag{13}$$

The above formulas do not take cohesive forces of clay soils into account. Therefore, when the soil is clay, internal forces generated by cohesive force c should be considered. The internal force $\sigma_c = c\cot\varphi$ produced by cohesive force c is regarded approximately as a uniform force on the boundary surfaces of the soils, substituting it into equation (13), the calculation formula for σ_z in clay soils can be obtained:

$$\sigma_z = \frac{\gamma}{A} - \left[\frac{\gamma}{A} - (q - c\cot\varphi)\right]e^{-Az} - c\cot\varphi. \tag{14}$$

3.3. Force Calculation of Front Walls Transmitted from Soils between Covered Piles. According to previous research results, the soil arch between piles can be divided into two parts, as shown in Figure 5.

The earth pressure in the distance is assumed to be transferred to adjacent covered piles through the outer arch area and stable inner arch area, and front sheet-pile walls can be used as a pair of parallel walls. When the pressure line of the arch coincides with the arch axis, the bending moment of each section is zero, and arches have no bending moment and the material cost is the most economical. Since the three-

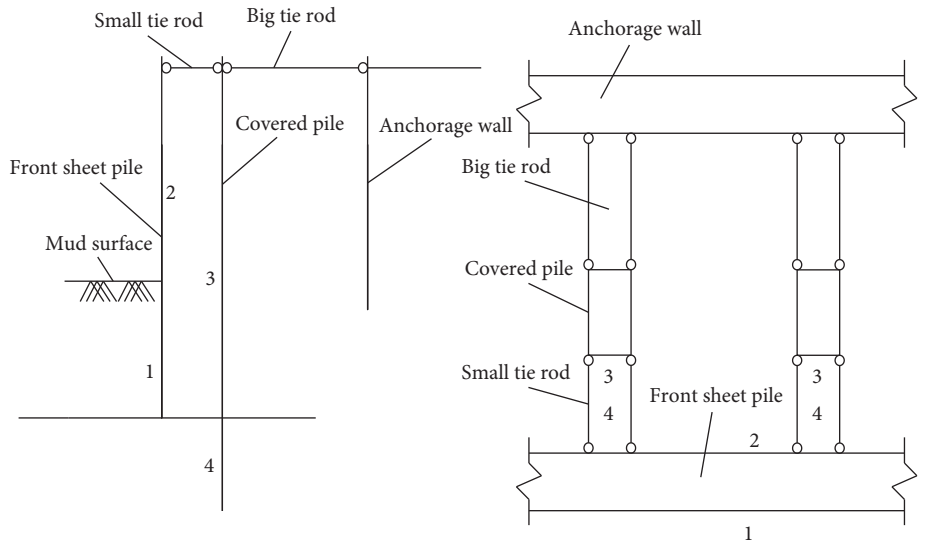

Figure 3: Structural calculation model of covered sheet-pile wharf.

Table 1: Reference values of lateral pressure coefficient K_w.

δ	φ										
	15°	18°	21°	24°	27°	30°	33°	36°	39°	42°	45°
0°	0.589	0.528	0.472	0.422	0.376	0.333	0.295	0.260	0.228	0.198	0.172
3°	0.592	0.530	0.474	0.423	0.376	0.334	0.295	0.260	0.228	0.198	0.172
6°	0.601	0.536	0.478	0.426	0.378	0.335	0.296	0.261	0.228	0.199	0.172
9°	0.618	0.547	0.486	0.431	0.382	0.338	0.298	0.262	0.229	0.200	0.173
12°	0.652	0.566	0.498	0.439	0.388	0.342	0.301	0.264	0.231	0.201	0.173
15°	0.784	0.601	0.517	0.452	0.396	0.348	0.305	0.267	0.233	0.202	0.174
18°		0.733	0.551	0.471	0.409	0.356	0.311	0.271	0.236	0.204	0.176
21°			0.682	0.504	0.427	0.368	0.319	0.276	0.239	0.207	0.178
24°				0.631	0.459	0.385	0.330	0.284	0.244	0.210	0.180
27°					0.581	0.415	0.346	0.294	0.251	0.214	0.183
30°						0.531	0.373	0.308	0.260	0.220	0.187
33°							0.482	0.334	0.273	0.228	0.192
36°								0.435	0.296	0.240	0.199
39°									0.390	0.261	0.210
42°										0.347	0.228
45°											0.306

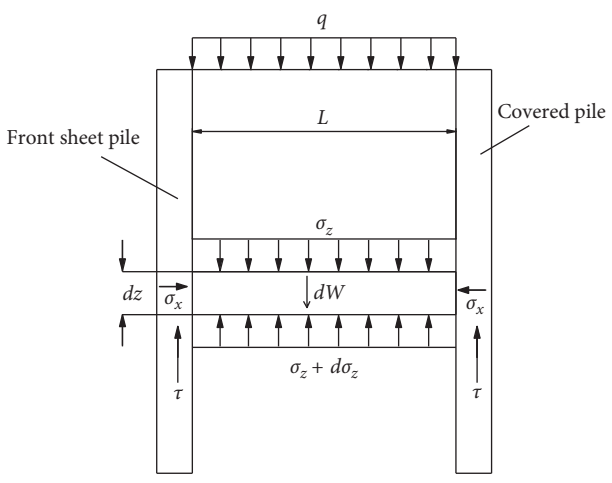

Figure 4: Diagram of soil calculation.

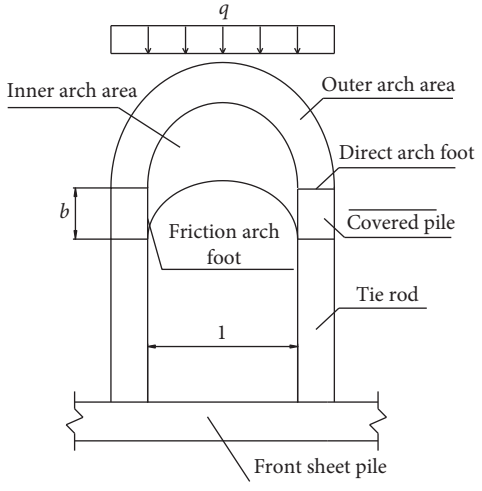

Figure 5: Diagram of arch area division.

hinged arch structure and loads are symmetrical, half of the three-hinged arch is considered as the research object. The coordinate system is set up as shown in Figure 6. The equation for a reasonable arch axis is

$$y = \frac{4f}{l^2}(l - x)x. \tag{15}$$

Reaction force of the arch foot:

$$R_x = \frac{ql^2}{8f}, \qquad R_y = \frac{ql}{2}. \tag{16}$$

Combined with $R_x = R_y \tan\delta$, the equation for the reasonable arch axis is calculated by

$$f = \frac{l}{4\tan\delta}, \tag{17}$$

where l is the arch span, f is the arch height, and δ is the friction angle.

Along the vertical direction, at any depth z, microsoil with a thickness of dz is taken, as shown in Figure 7. Forces acting on microsoils in the vertical direction are as follows:

Gravity:

$$W = \gamma s\, dz, \tag{18}$$

where $s = (L + f)l$.

Friction between the soils and front sheet-pile walls:

$$T_\delta = l\tau_\delta\, dz = l\, dz\sigma_y \tan\delta. \tag{19}$$

Soil friction at soil arches:

$$T_\varphi = l\tau_\varphi\, dz = l\, dz\sigma_y \tan\varphi. \tag{20}$$

Earth pressure difference between the upper and lower surfaces:

$$\Delta p = (\sigma_z + d\sigma_z - \sigma_z)s. \tag{21}$$

Vertical force equilibrium equation of microsoils:

$$T_\delta + T_\varphi + (\sigma_z + d\sigma_z - \sigma_z)s = W, \tag{22}$$

where σ_z and σ_y are the vertical stress and horizontal stress, respectively.

The forces transmitted from the soils in the arches to the front sheet-pile walls are assumed to be evenly distributed on the horizontal plane. Forces are distributed in the vertical direction according to lateral pressure coefficient $K_w = \sigma_y/\sigma_z$. Combined with the above formulas, the following formula is obtained:

$$\gamma\, dz = d\sigma_z + \frac{4K_w \tan\delta(\tan\delta + \tan\varphi)}{4L\tan\delta + l}\sigma_z\, dz. \tag{23}$$

According to the analytic theory of differential equations, the following formula can be obtained:

$$\sigma_z = \frac{\gamma}{B} + Ce^{-Az}, \tag{24}$$

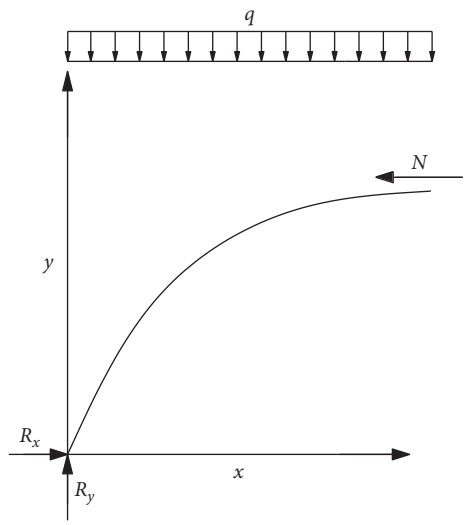

Figure 6: Diagram of soil arch subjected to forces.

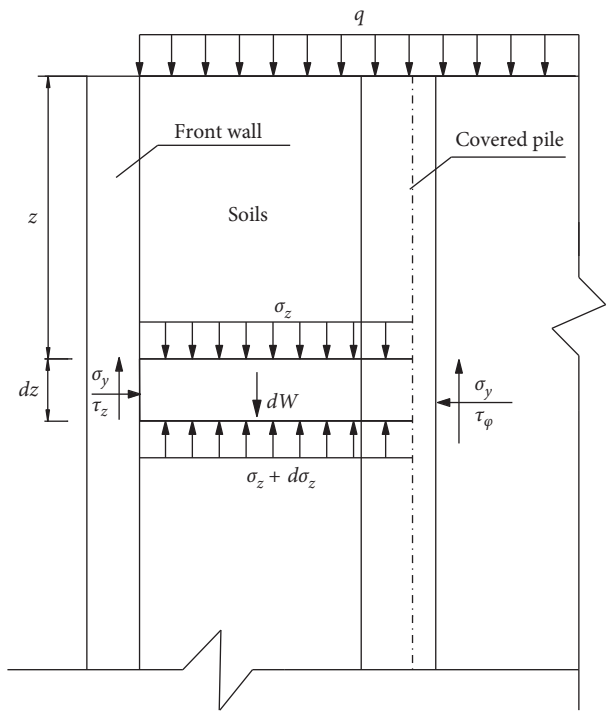

Figure 7: Soil force state considering arching effect.

Boundary condition:

$$\sigma_{z=0} = q. \tag{25}$$

Substituting equation (25) into equation (24), the following formula is obtained:

$$C = q - \frac{\gamma}{B}, \tag{26}$$

$$\text{Therefore:}\quad \sigma_z = \frac{\gamma}{B}\left(1 - e^{-Az}\right) + qe^{-Az}. \tag{27}$$

The above formulas do not take cohesive forces of clay soils into account. Therefore, when the soil is clay, the

internal forces generated by cohesive force c should be considered. The internal force $\sigma_c = c\cot\varphi$ produced by cohesive force c is considered an approximately uniform force on the boundary surfaces of the soils. Substituting this force into equation (27), the calculation formula for σ_z in clay soils can be obtained:

$$\sigma_z = \frac{\gamma}{B} - \left[\frac{\gamma}{B} - (q - c\cot\varphi)\right]e^{-Az} - c\cot\varphi. \tag{28}$$

The earth pressure on the front sheet-pile walls, which are close to land, is calculated by

$$\sigma_y = K_w\left\{\frac{\gamma}{B} - \left[\frac{\gamma}{B} - (q - c\cot\varphi)\right]e^{-Az} - c\cot\varphi\right\}. \tag{29}$$

3.4. Earth Pressure on Front Sheet-Pile Walls beneath Mud Surface. When calculating the earth pressure on the front sheet-pile walls, which are below the mud surface, considering the stiffness of the covered sheet-pile wharves under static loads is large but the horizontal displacement generated by the structure is relatively small, and an elastic resistance method is adopted, that is, the soil horizontal resistance at any depth z is proportional to the soil horizontal displacement y, that is,

$$P_z = K(h)y. \tag{30}$$

Currently, the "m" method is adopted in port engineering in China to determinate the horizontal resistance coefficient K_Z. Assuming the earth resistance coefficient increases linearly with depth,

$$K(h) = mh. \tag{31}$$

Substituting equation (31) into equation (30), P_z is computed by

$$P_z = mhy = m(z - h_1)y. \tag{32}$$

3.5. Earth Pressure on Front Sheet-Pile Walls above Mud Surface. The displacement calculation for front sheet-pile walls of covered sheet-pile wharves is the same as for traditional sheet-pile wharves. Since the stress characteristics and deformation mechanism of front sheet-pile walls, which are in soils, are completely different from those above the mud surface, the front sheet-pile wall is divided into upper and lower parts at the mud surface for separate calculations. Below the mud surface, the sheet-pile walls can be simplified as elastic structures buried in soil, with the top layer being flat with the mud surface. The pile top has moment M_0 and lateral force Q_0. M_0 and Q_0 are the resultant moment and force of the sheet-pile wall mud surface from the force above the sheet-pile wall mud surface. The rotation angle and displacement of the pile top are φ_0 and y_0, respectively. According to the previous description, when a pile lateral displacement y occurs at depth z, the soil resistance force acting on the piles at depth z is

$$P_z = K(h)yb_0 = m(z - H_1)yb_0. \tag{33}$$

The overloaded soil pressure and residual water pressure above the mud surface are assumed to be uniform external loads. The overloaded soil pressure is averagely distributed according to the soil width between covered piles and behind covered piles and has a value q' that is calculated by

$$q' == \frac{\sigma_{xn}b + \sigma_{yn}l_1}{b + l_1} - \frac{c_n}{\tan\varphi_n}(1 - K_w), \tag{34}$$

where b is the covered pile width (m), l_1 is the covered pile net distance (m), σ_{yn} is the horizontal earth pressure generated by soils between covered piles and front sheet-pile walls at the mud surface, and c_n and φ_n are the cohesive force (kPa) and the internal friction angle (°) at the mud surface, respectively.

Considering the conversion depth ($\overline{h} = \alpha(z - H_1)$), based on the deflection curve differential equation in material mechanics, the following formulas are obtained:

$$EI\frac{d^4y}{d\overline{h}^4} = -P_Z + q'. \tag{35}$$

Substituting equation (33) into equation (35),

$$EI\frac{d^4y}{d\overline{h}^4} = -m\overline{h}yb_0 + q'. \tag{36}$$

Boundary conditions:

$$\begin{aligned} y_{(\overline{h}_0)} &= y_0, \\ \frac{dy}{d\overline{h}_{(z=H_1)}} &= \varphi_0, \\ EI\frac{d^2y}{d\overline{h}^2_{(\overline{h}_0)}} &= M_0, \\ EI\frac{d^3y}{d\overline{h}^3_{(z=H_1)}} &= Q_0. \end{aligned} \tag{37}$$

According to the analytical theory of differential equations, the solution of equation (36) can be expressed by the following power series:

$$y = \sum_{i=0}^{\infty}\alpha_i\overline{h}^i. \tag{38}$$

The following formula can be obtained by derivation:

$$y = y_0A_1 + \frac{\varphi_0}{\alpha}B_1 + \frac{M_0}{\alpha^2EI}C_1 + \frac{Q_0}{\alpha^3EI}D_1 + \frac{q'}{\alpha^4EI}E_1, \tag{39}$$

$$M = \alpha^2EIy_0A_3 + \alpha EI\varphi_0B_3 + M_0C_3 + \frac{Q_0}{\alpha}D_3 + \frac{q'}{\alpha^2}E_3, \tag{40}$$

$$Q = \alpha^3EIy_0A_4 + \alpha^2EI\varphi_0B_4 + \alpha M_0C_4 + Q_0D_4 + \frac{q'}{\alpha}E_4. \tag{41}$$

Combined with the bottom boundary conditions: $M = 0$, $Q = 0$, the initial displacement y_0 and initial rotation angle φ_0 at the mud surface are calculated separately as

$$y_0 = \frac{M_0}{\alpha^2 EI}\left(\frac{B_4C_3 - B_3C_4}{A_4B_3 - A_3B_4}\right) + \frac{Q_0}{\alpha^3 EI}\left(\frac{B_4D_3 - B_3D_4}{A_4B_3 - A_3B_4}\right) + \frac{q'}{\alpha^4 EI}\left(\frac{B_4E_3 - B_3E_4}{A_4B_3 - A_3B_4}\right), \tag{42}$$

$$\varphi_0 = \frac{M_0}{\alpha EI}\left(\frac{A_4C_3 - A_3C_4}{A_3B_4 - A_4B_3}\right) + \frac{Q_0}{\alpha^2 EI}\left(\frac{A_4D_3 - A_3D_4}{A_3B_4 - A_4B_3}\right) + \frac{Q_0}{\alpha^2 EI}\left(\frac{A_4D_3 - A_3D_4}{A_3B_4 - A_4B_3}\right). \tag{43}$$

The shear force Q_0 and bending moment M_0 of front sheet-pile walls at the mud surface should be calculated accumulatively:

$$Q_0 = R_a - \frac{b\sum_{i=1}^{n}\int_{z_{i-1}}^{z_i}\sigma_x\,dz + l\sum_{i=1}^{n}\int_{z_{i-1}}^{z_i}\sigma_y\,dz}{b+l}, \tag{44}$$

$$M_0 = R_a(H_1 - h_0) - \frac{b\sum_{i=1}^{n}l_i\int_{z_{i-1}}^{z_i}\sigma_x\,dz + l\sum_{i=1}^{n}l_i\int_{z_{i-1}}^{z_i}\sigma_y\,dz}{b+l}, \tag{45}$$

where z_i is the distance from the bottom of the i-th layer to the wharf surface (m), l_i is the distance from the earth pressure point of the i-th layer to the front mud surface (m).

3.6. Displacement Calculation of Front Wall When Anchorage Point Displacement Is Ignored. The dynamic water load is a variable parameter and it is also helpful to reduce the displacement of the front wall sheet-pile wharf. Therefore, in the paper, the calculation method of displacement on front wall was deduced considering the most dangerous situation without dynamic water load.

When the strength of the covered pile or anchorage structure is sufficient, the displacement of the upper part of front sheet-pile walls is smaller, displacement in the middle and lower part is larger, front sheet-pile walls tend to rotate around the anchorage point, and displacement at the anchorage point is negligible compared to the bottom displacement. Displacement at the anchorage point is assumed to be zero when tie rod tension and front wall displacement are solved, and the solution process is as follows.

The displacement of the front sheet-pile wall at the anchorage point primarily consists of four parts: displacement y_0 at the mud surface, displacement caused by rotation φ_0 at the mud surface, displacement Δ of front sheet-pile wall at the anchorage point caused by earth pressure behind the wall, and displacement f of front sheet-pile wall at the anchorage point caused by tie rod tension. Displacement of the front sheet-pile wall at the anchorage point is assumed to be zero. The following formula is obtained:

$$y_0 + \varphi_0(H_1 - h_0) + \Delta + f = 0. \tag{46}$$

(1) Calculate displacement f.

According to material mechanics formula:

$$M_h = EI\frac{d^2y}{dh^2} = R_a(H_1h_0 - h), \quad 0 \le h \le H_1 - h_0. \tag{47}$$

Boundary conditions:

$$\begin{cases} \varphi_{(h=0)} = 0, \\ y_{(h=0)} = 0. \end{cases} \tag{48}$$

Combined with the boundary conditions, the formula solution is expressed by

$$\begin{cases} y = \dfrac{R_a h^2}{6EI}\left[3(H_1 - h_0) - h\right], & (0 \le h \le H_1 - h_0), \\ y = \dfrac{R_a(H_1 - h_0)^2}{6EI}\left[3h - (H_1 - h_0)\right], & (H_1 - h_0 \le h \le H_1). \end{cases} \tag{49}$$

Converting equation (49) to a formula with depth z as a variable, the formula is expressed by

$$\begin{cases} y = \dfrac{R_a(H_1 - Z)^2}{6EI}\left[3(H_1 - h_0) - (H_1 - z)\right], & (h_0 \le z \le H_1), \\ y = \dfrac{R_a(H_1 - h_0)^2}{6EI}\left[3(H_1 - z) - (H_1 - h_0)\right], & (0 \le z \le h_0). \end{cases} \tag{50}$$

Displacement f is expressed by

$$f = y_{(z=h_0)} = \frac{R_a(H_1 - h_0)^3}{3EI}. \tag{51}$$

(2) Calculate displacement Δ.

According to the material mechanics formula:

$$EI\frac{d^2y}{dz^2} = \frac{b\int_0^z\sigma_x(H_1 - z)\,dz + l\int_0^z\sigma_y(H_1 - z)\,dz - (H_1 - z)\left(b\int_0^z\sigma_x\,dz + l\int_0^z\sigma_y\,dz\right)}{b+l}. \tag{52}$$

Boundary conditions:

$$\begin{cases} \varphi_{(z=H_1)} = EI\dfrac{dy}{dz_{z=h_1}} = 0, \\ y_{(z=H_1)} = 0. \end{cases} \tag{53}$$

In summary, displacement f and Δ are expressed by

$$y = \frac{-1}{EI(b+l)}\left\{\frac{K_w}{\overline{A}}\left[\frac{\overline{\gamma}}{\overline{A}} - (q - \overline{c}\cot\overline{\varphi})\right]\left(-\frac{bz^3}{6} + \frac{bz^3}{2\overline{A}} - \frac{b}{\overline{A}^3}e^{-\overline{A}z} + \frac{bzH_1^2}{2} - \frac{bzH_1}{\overline{A}} - \frac{bz}{\overline{A}^2}e^{-\overline{A}H_1} - \frac{bH_1^3}{3} + \frac{bH_1^2}{2\overline{A}} + \frac{b}{\overline{A}^3}e^{-\overline{A}H_1}\right.\right.$$
$$\left. + \frac{bH_1}{\overline{A}^2}e^{-\overline{A}H_1}\right) + \frac{K_w}{\overline{A}}\left[\frac{\overline{\gamma}}{\overline{B}} - (q - \overline{c}\cot\overline{\varphi})\right]\left(-\frac{lz^3}{6} + \frac{lz^2}{2\overline{A}} - \frac{l}{\overline{A}^3}e^{-\overline{A}z} + \frac{lH_1^2 z}{2} - \frac{lzH_1}{\overline{A}} - \frac{lz}{\overline{A}^2}e^{-\overline{A}H_1} - \frac{lH_1^3}{3} + \frac{lH_1^2}{2\overline{A}} + \frac{l}{\overline{A}^3}e^{-\overline{A}H_1} + \frac{lH_1}{\overline{A}^2}e^{-\overline{A}H_1}\right)$$
$$+ \frac{1}{24}bK_w\frac{\overline{\gamma}}{\overline{A}}z^4 - \frac{bK_w z\overline{\gamma}H_1^3}{6\overline{A}} + \frac{bK_w\overline{\gamma}H_1^4}{8\overline{A}} + \frac{1}{24}lK_w\frac{\overline{\gamma}}{\overline{B}}z^4 - \frac{lK_w z\overline{\gamma}H_1^3}{6\overline{B}} + \frac{lK_w\overline{\gamma}H_1^4}{8\overline{B}} - \frac{bcK_w\cot\overline{\varphi}z^4}{24} + \frac{bczK_w\cot\overline{\varphi}H_1^3}{6}$$
$$\left. - \frac{bcK_w\cot\overline{\varphi}H_1^4}{8} - \frac{lcK_w\cot\overline{\varphi}z^4}{24} + \frac{lczK_w\cot\overline{\varphi}H_1^3}{6} - \frac{lcK_w\cot\overline{\varphi}H_1^4}{8}\right\}, \tag{54}$$

$$\Delta = \frac{-1}{EI(b+l)}\left\{\frac{K_w}{\overline{A}}\left[\frac{\overline{\gamma}}{\overline{A}} - (q - \overline{c}\cot\overline{\varphi})\right]\left(-\frac{bh_0^3}{6} + \frac{bh_0^2}{2\overline{A}} - \frac{b}{\overline{A}^3}e^{-\overline{A}h_0} + \frac{bh_0H_1^2}{2} - \frac{bh_0H_1}{\overline{A}} - \frac{bh_0}{\overline{A}^2}e^{-\overline{A}H_1} - \frac{bH_1^3}{3} + \frac{bH_1^2}{2\overline{A}} + \frac{b}{\overline{A}^3}e^{-\overline{A}H_1}\right.\right.$$
$$\left. + \frac{bH_1}{\overline{A}^2}e^{-\overline{A}H_1}\right) + \frac{K_w}{\overline{A}}\left[\frac{\overline{\gamma}}{\overline{B}} - (q - \overline{c}\cot\overline{\varphi})\right]\left(-\frac{lh_0^3}{6} + \frac{lh_0^2}{2\overline{A}} - \frac{l}{\overline{A}^3}e^{-\overline{A}h_0} + \frac{lH_1^2h_0}{2} - \frac{lh_0H_1}{\overline{A}} - \frac{lh_0}{\overline{A}^2}e^{-\overline{A}H_1} - \frac{lH_1^3}{3} + \frac{lH_1^2}{2\overline{A}} + \frac{l}{\overline{A}^3}e^{-\overline{A}H_1}\right.$$
$$\left. + \frac{lH_1}{\overline{A}^2}e^{-\overline{A}H_1}\right) + \frac{1}{24}bK_w\frac{\overline{\gamma}}{\overline{A}}h_0^4 - \frac{bK_wh_0\overline{\gamma}H_1^3}{6\overline{A}} + \frac{bK_w\overline{\gamma}H_1^4}{8\overline{A}} + \frac{1}{24}lK_w\frac{\overline{\gamma}}{\overline{B}}h_0^4 - \frac{lK_wh_0\overline{\gamma}H_1^3}{6\overline{B}} + \frac{lK_w\overline{\gamma}H_1^4}{8\overline{B}} - \frac{bcK_w\cot\overline{\varphi}z^4}{24}$$
$$\left. + \frac{bch_0K_w\cot\overline{\varphi}H_1^3}{6} - \frac{bcK_w\cot\overline{\varphi}H_1^4}{8} - \frac{lcK_w\cot\overline{\varphi}h_0^4}{24} + \frac{lczK_w\cot\overline{\varphi}H_1^3}{6} - \frac{lcK_w\cot\overline{\varphi}H_1^4}{8}\right\}. \tag{55}$$

The displacement at any point of the front sheet-pile wall above the mud surface can be expressed by

$$y = y_0 + \varphi_0(H_1 + z) + \Delta_z + f_z. \tag{56}$$

Finally, formulas to calculate the displacement of any point on the front sheet-pile wall above the mud surface can be expressed by

$$y = y_0 + \varphi_0(H_1 + z) + \Delta_z + f_z,$$

$$y_0 = \frac{M_0}{\alpha^2 EI}\left(\frac{B_4C_3 - B_3C_4}{A_4B_3 - A_3B_4}\right) + \frac{Q_0}{\alpha^3 EI}\left(\frac{B_4D_3 - B_3D_4}{A_4B_3 - A_3B_4}\right) + \frac{q'}{\alpha^4 EI}\left(\frac{B_4E_3 - B_3E_4}{A_4B_3 - A_3B_4}\right),$$

$$\varphi_0 = \frac{M_0}{\alpha EI}\left(\frac{A_4C_3 - A_3C_4}{A_3B_4 - A_4B_3}\right) + \frac{Q_0}{\alpha^2 EI}\left(\frac{A_4D_3 - A_3D_4}{A_3B_4 - A_4B_3}\right) + \frac{q'}{\alpha^3 EI}\left(\frac{A_4E_3 - A_3E_4}{A_3B_4 - A_4B_3}\right),$$

$$\Delta_z = \frac{-1}{EI(b+l)}\left\{\frac{K_w}{\overline{A}}\left[\frac{\overline{\gamma}}{\overline{A}} - (q - \overline{c}\cot\overline{\varphi})\right]\left(-\frac{bh_0^3}{6} + \frac{bh_0^2}{2\overline{A}} - \frac{b}{\overline{A}^3}e^{-\overline{A}z} + \frac{bzH_1^2}{2} - \frac{bzH_1}{\overline{A}} - \frac{bz}{\overline{A}^2}e^{-\overline{A}H_1} - \frac{bH_1^3}{3} + \frac{bH_1^2}{2\overline{A}} + \frac{b}{\overline{A}^3}e^{-\overline{A}H_1}\right.\right.$$
$$\left. + \frac{bH_1}{\overline{A}^2}e^{-\overline{A}H_1}\right) + \frac{K_w}{\overline{A}}\left[\frac{\overline{\gamma}}{\overline{B}} - (q - \overline{c}\cot\overline{\varphi})\right]\left(-\frac{lz^3}{6} + \frac{lz^2}{2\overline{A}} - \frac{l}{\overline{A}^3}e^{-\overline{A}z} + \frac{lH_1^2z}{2} - \frac{lzH_1}{\overline{A}} - \frac{lz}{\overline{A}^2}e^{-\overline{A}H_1} - \frac{lH_1^3}{3} + \frac{lH_1^2}{2\overline{A}} + \frac{l}{\overline{A}^3}e^{-\overline{A}H_1}\right.$$
$$\left. + \frac{lH_1}{\overline{A}^2}e^{-\overline{A}H_1}\right) + \frac{1}{24}bK_w\frac{\overline{\gamma}}{\overline{A}}z^4 - \frac{bK_wz\overline{\gamma}H_1^3}{6\overline{A}} + \frac{bK_w\overline{\gamma}H_1^4}{8\overline{A}} + \frac{1}{24}lK_w\frac{\overline{\gamma}}{\overline{B}}z^4 - \frac{lK_wz\overline{\gamma}H_1^3}{6\overline{B}} + \frac{lK_w\overline{\gamma}H_1^4}{8\overline{B}} - \frac{bcK_w\cot\overline{\varphi}z^4}{24}$$
$$\left. + \frac{bczK_w\cot\overline{\varphi}H_1^3}{6} - \frac{bcK_w\cot\overline{\varphi}H_1^4}{8} - \frac{lcK_w\cot\overline{\varphi}z^4}{24} + \frac{lczK_w\cot\overline{\varphi}H_1^3}{6} - \frac{lcK_w\cot\overline{\varphi}H_1^4}{8}\right\},$$

$$f_z = \begin{cases} y = \dfrac{R_a(H_1 - Z)^2}{6EI}\left[3(H_1 - h_0) - (H_1 - z)\right], & (h_0 \le z \le H_1), \\ y = \dfrac{R_a(H_1 - h_0)^2}{6EI}\left[3(H_1 - z) - (H_1 - h_0)\right], & (0 \le z \le h_0). \end{cases} \tag{57}$$

3.7. Considering Displacement of Anchorage Point to Calculate Front Wall Displacement. When the strength of the covered pile or anchorage structure is insufficient, the displacement of the upper part of the front sheet-pile walls is larger, displacement at the bottom part is smaller, front sheet-pile walls tend to rotate around the front sheet-pile wall bottom, and displacement at the anchorage point is not negligible. The displacement at the anchorage point is assumed to have a specific value when the tie rod tension and front wall displacement are calculated, and the solution process is as follows.

The displacement at the anchorage point is y_a. Substituting this into equation (57),

$$\varphi_0 = \frac{M_0}{\alpha EI}\left(\frac{A_4C_3 - A_3C_4}{A_3B_4 - A_4B_3}\right) + \frac{Q_0}{\alpha^2 EI}\left(\frac{A_4D_3 - A_3D_4}{A_3B_4 - A_4B_3}\right) + \frac{q'}{\alpha^3 EI}\left(\frac{A_4E_3 - A_3E_4}{A_3B_4 - A_4B_3}\right),$$

$$\Delta_z = -\frac{1}{EI}\left[\frac{1}{120}\overline{\gamma}\overline{k}z^5 + \frac{1}{24}\overline{\gamma}\overline{k}H_1^4(H_1 - z) - \frac{1}{120}\overline{\gamma}\overline{k}H_1^5\right], \tag{58}$$

the following equation is obtained:

$$y_0 = \varphi_0(H_1 - h_0) + \Delta + f = y_a. \tag{59}$$

The following formula is recommended to determine y_a:

$$y_a = \frac{(H_1 - h_0)y_0}{H_2}. \tag{60}$$

Displacement at any point of the front sheet-pile walls above the mud surface can be expressed by

$$y = y_0 + \varphi_0(H_1 - z) + \Delta_z + f_z. \tag{61}$$

Finally, the displacement at any point above the mud surface of the front sheet-pile walls can be expressed by

$$y = y_0 + \varphi_0(H_1 - z) + \Delta_z + f_z,$$

$$y_0 = \frac{M_0}{\alpha^2 EI}\left(\frac{B_4C_3 - B_3C_4}{A_4B_3 - A_3B_4}\right) + \frac{Q_0}{\alpha^3 EI}\left(\frac{B_4D_3 - B_3D_4}{A_4B_3 - A_3B_4}\right) + \frac{q'}{\alpha^4 EI}\left(\frac{B_4E_3 - B_3E_4}{A_4B_3 - A_3B_4}\right),$$

$$f_z = \begin{cases} y = \dfrac{R_a(H_1 - Z)^2}{6EI}\left[3(H_1 - h_0) - (H_1 - z)\right], & (h_0 \le z \le H_1), \\ y = \dfrac{R_a(H_1 - h_0)^2}{6EI}\left[3(H_1 - z) - (H_1 - h_0)\right], & (0 \le z \le h_0). \end{cases} \tag{62}$$

3.8. Flow Chart of Front Wall Displacement Calculation. A flow chart of the displacement calculation process for the front walls of covered sheet-pile wharves under static loads is shown in Figure 8.

4. Example of Displacement Calculation for Front Wall of Covered Sheet-Pile Wharf

4.1. Project Overview. The calculation model is based on the Jingtang Port 32# wharf. The front walls and anchorage wall structure are continuous underground walls. The distance between covered piles is 1.2 m, and the cross-sectional form is shown in Figure 9. The soil, wall, and tie rod parameters are shown in Table 2.

The Nanjing Hydraulic Research Institute organized relevant personnel to complete the installation of the instrumentation in February 2005, and the observation period was from June 2005 to February 2008. The observation results are shown in Table 3.

4.2. Theoretical Calculation Results. According to the displacement calculation theory for the front wall of a covered sheet-pile wharf under static loads, the displacement of the front wall when displacement at the anchorage point is neglected or considered is shown in Table 4.

4.3. Comparison and Analysis of Calculation Results. The theoretical calculation and in situ measurement results for the front sheet-pile wall displacement of a covered sheet-pile wharf are shown in Figure 10.

From the figure, whether the displacement at the anchor point is considered or neglected has little effect on the displacement calculation of the front sheet-pile wall, which is below the mud surface. The results obtained using two calculation methods are close to measured data. The results of the two calculation methods are very different when calculating the displacement of the front sheet-pile wall, which is below the mud surface. When displacement at the anchorage point is ignored, the displacement at the anchorage point is limited artificially; therefore, the calculation result of tie rod tension is relatively large, which leads to the displacement calculation of the front wall above the mud surface being greatly reduced. The deformation mode of the front sheet-pile wall is a middle convex drum, and the maximum displacement is approximately 20 mm, which is very different from actual in situ measurement results.

When considering displacement at the anchorage point, the calculated tie rod tension is more accurate and the front wall displacement calculation is very close to the in situ measurement result because the anchorage point displacement is assumed scientifically. The upper part of the front wall is partially

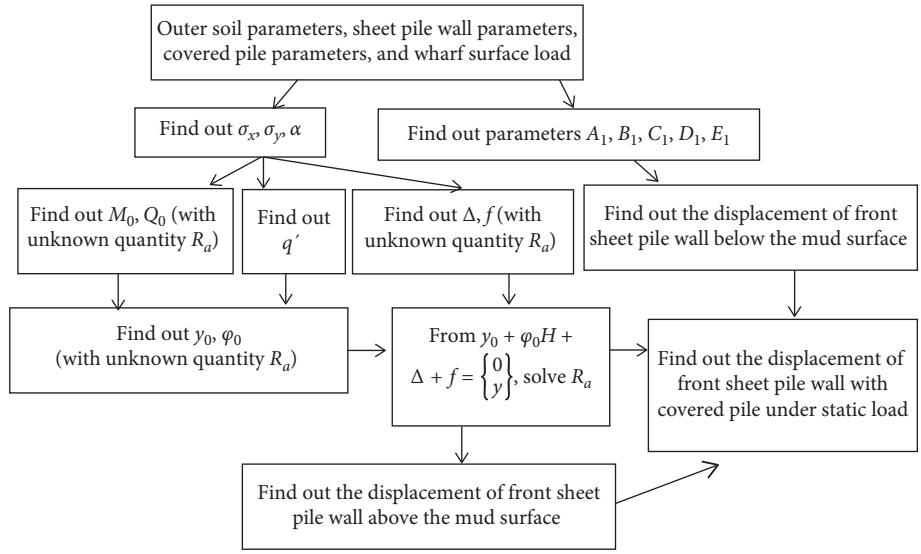

Figure 8: Flow chart of displacement calculation process for the front walls of covered sheet-pile wharves under static loads.

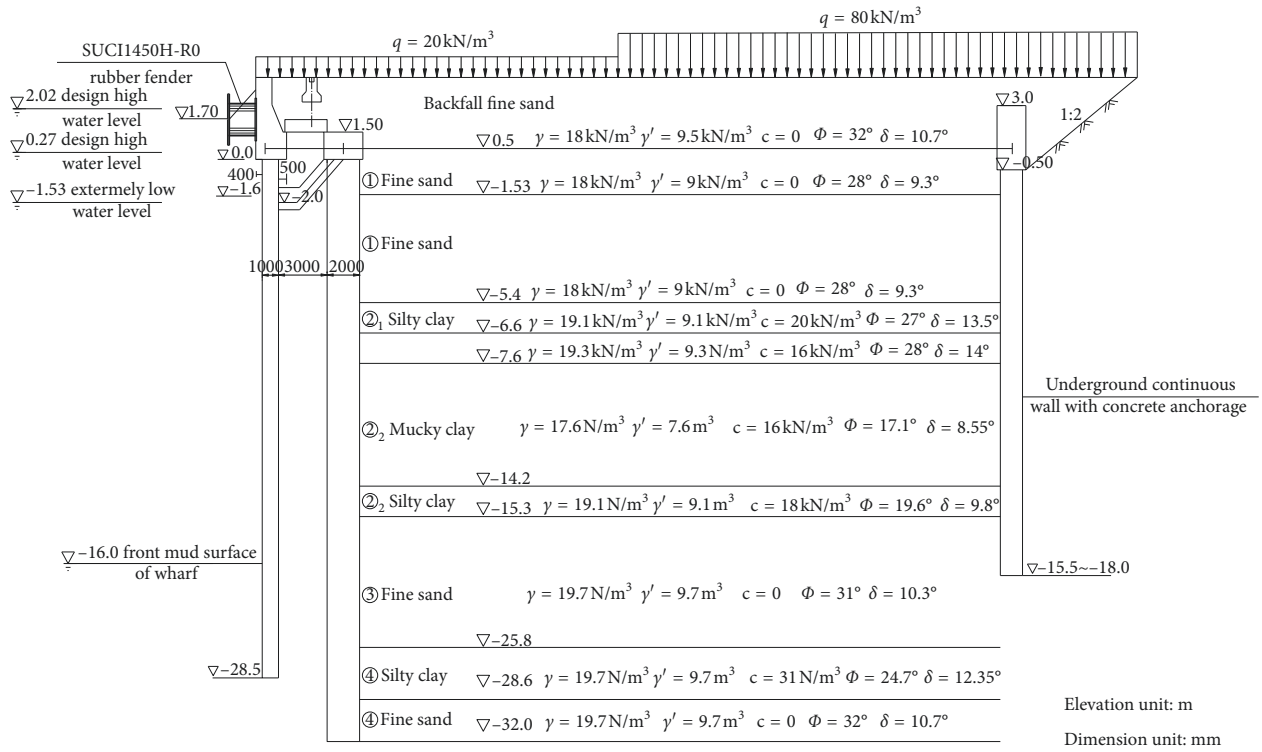

Figure 9: Schematic diagram of Jingtang Port 32# wharf.

restrained in an inclined deformation mode. The maximum displacement at the anchorage point of the front wall is approximately 55 mm, the measured maximum displacement is approximately 60 mm, and the error is 8.33%, which is ideal. In conclusion, it is more scientific to use the hypothetical anchorage point displacement proposed in this paper.

5. Conclusion

This paper is based on the theory of soil pressure and the soil arching effect. According to the stress and deformation characteristics of a covered sheet-pile wharf, the formulas used to calculate the force and deformation of the front wall of a covered sheet-pile wharf under static loads are deduced, and a comparison of actual measured stress and deformation data of Jingtang Port 32# is used to verify the accuracy of the theoretical derivation. The comparison shows that when calculating the displacement of the front sheet-pile wall, which is below the mud surface, the results of the two methods are not very different and are in good agreement with field measured data. However, when the displacement of the front sheet-pile wall is calculated, which is above the

Table 2: Soil, wall, and tie rod parameters.

Material type	Unit weight (kN/m^3)	Angle of internal friction (°)	Cohesion (kPa)	Elastic modulus (MPa)	Poisson's ratio
Soil layer 1	18.0	32.0	5	26.00	0.29
Soil layer 2	18.0	28.0	5	26.00	0.29
Soil layer 3	19.1	27.0	20	8.97	0.30
Soil layer 4	19.3	28.0	16	12.60	0.30
Soil layer 5	17.6	17.1	16	3.60	0.30
Soil layer 6	19.1	19.6	18	8.97	0.30
Soil layer 7	19.7	31.0	5	26.00	0.29
Soil layer 8	19.7	24.7	31	8.97	0.30
Soil layer 9	19.7	32.0	5	26.00	0.29
Concrete	25.0	—	—	2.80×10^4	0.20
Steel tie rod	78.5	—	—	2.06×10^5	0.20

Table 3: In situ measured data.

Observation cross section and calculation conditions		Bending moment of front wall (kN·m)		Anchorage wall (kN·m)	Bending moment Pile (kN·m)		Tension of tie rod (kN)	Displacement of anchorage point (cm)
		Maximum positive bending moment	Maximum negative bending moment	Maximum negative bending moment	Maximum positive bending moment	Maximum negative bending moment		
Observation cross section	#2	813	−1119	−762	1735	−2001	601	6.2
	#3	682	−936	−847	1907	−2054	526	
	#4	845	−839	−627	2180	−1823	446	4.7
Result	Condition 2	774	−700	−765	2739	−1988	636	9.0
	Condition 4	548	−568	−766	1713	−1713	433	6.5

Table 4: Data for displacement of front pile wall.

Neglecting displacement of anchorage point		Considering displacement of anchorage point	
Variable	Value	Variable	Value
α	0.255	α	0.255
q'	−45.025	q'	−45.025
Q_0	−119.445	Q_0	−154.785
M_0	44.788	M_0	−538.322
φ_0	0.001759	φ_0	0.003503
y_0	−0.016669	y_0	−0.023716
R_a	187.218	R_a	151.878
$y_{z=22.2}$	−0.013	$y_{z=22.2}$	−0.0172
$y_{z=24.2}$	−0.010	$y_{z=24.2}$	−0.0118
$y_{z=26.2}$	−0.007	$y_{z=26.2}$	−0.00782
$y_{z=28.2}$	−0.005017	$y_{z=28.2}$	−0.00491
$y_{z=30.2}$	−0.00204	$y_{z=30.2}$	−0.00167
$y_{z=32.2}$	0.002316	$y_{z=32.2}$	0.00267
$y_{z=32.7}$	0.003769	$y_{z=32.7}$	0.00410
Displacement formula of front wall above mud surface		Displacement formula of front wall below mud surface	
$y = -1.002 \times 10^{-6}z^4 + 1.0106 \times 10^{-4}z^3 + 0.222z - 5.630 \times 10^{-3}z^2 + 4.587 \times e^{-0.049z} - 4.576$		$y = -1.002 \times 10^{-6}z^4 + 9.896 \times 10^{-5}z^3 + 0.225z - 5.606 \times 10^{-3}z^2 + 4.587 \times e^{-0.049z} - 4.643$	

Note. The unit of force is kN; the unit of length is m; the unit of torque is kN·m.

mud surface, and when displacement at the anchorage point is ignored, displacement at the anchorage point is limited artificially. Therefore, the result of tie rod tension is relatively large, which leads to the calculated displacement of the front

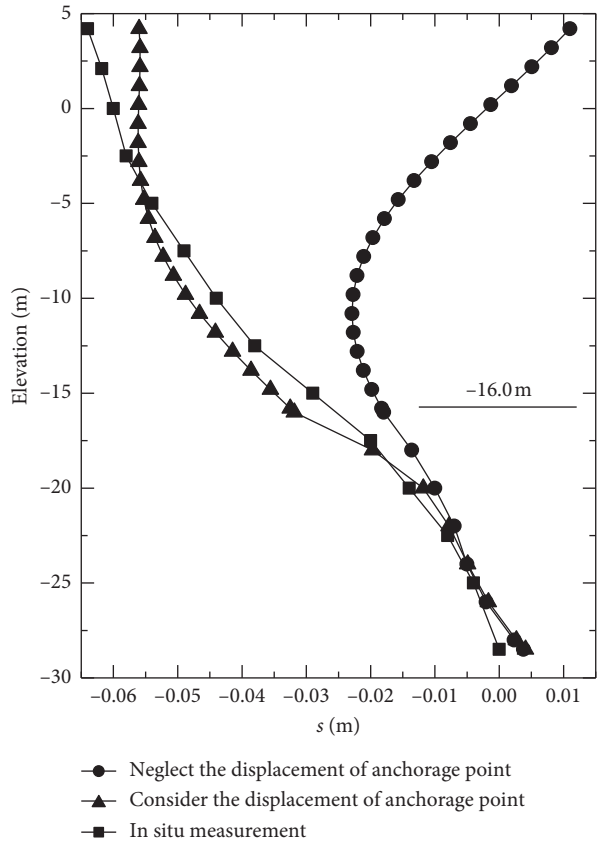

Figure 10: Comparison of two methods and measured data.

sheet-pile wall, which is above the mud surface, being greatly reduced. The deformation mode of the front sheet-pile wall is a middle convex drum, and the maximum displacement is approximately 20 mm, which is very different from the actual in situ measurement results. When displacement at the anchorage point is considered, the calculated tie rod tension is more accurate, and the results of the front wall displacement are very close to in situ measurement results because displacement at the anchorage point is assumed scientifically. The upper part of the front wall is partially restrained in an inclined deformation mode. The maximum displacement at the anchorage point of the front wall is approximately 55 mm, the measured maximum displacement is approximately 60 mm, and the error is 8.33%, which is ideal. In conclusion, it is more scientific to use the hypothetical anchorage point displacement proposed in this paper.

Data Availability

The data used to support the findings of this study are available from the corresponding author upon request.

Conflicts of Interest

The authors declare that there are no conflicts of interest regarding the publication of this paper.

Acknowledgments

This research was financially supported by the Natural Science Foundation of Jiangsu Province (Grant no. BK20161360), Six Major Talents Peak in Jiangsu Province in China (Grant no. 2016-JZ-020), and Postgraduate Research & Practice Innovation Program of Jiangsu Province (Grant no. SJCX17_0609).

References

[1] Y. X. Liu and Z. D. Wu, "Working mechanism of sheet pile wharf with barrier piles," *Hydro-Scienceand Engineering*, vol. 2, pp. 8–12, 2006.

[2] W. P. Liu, Y. R. Zheng, Z. Y. Cai, and Z. B. Jiao, "Finite element method for covered sheet pile wharves," *Chinese Journal of Geotechnical Engineering*, vol. 32, no. 4, pp. 573–577, 2010.

[3] W. C. Dong, "Practice in construction of deep water sheet-pile diaphragm-wall wharves in Jingtang port and experiential study," *Port Engineering Technology*, vol. 12, pp. 20–24, 2005.

[4] Y. Yu, "Generation and study on proposal of covered type of sheet pile wharf," *Port Engineering Technology*, no. S1, pp. 30–32, 2005.

[5] L. Y. Wang, H. L. Liu, P. M. Jiang, and X. X. Chen, "Prediction method of seismic residual deformation of caisson quay wall in liquefied foundation," *China Ocean Engineering*, vol. 25, no. 1, pp. 45–58, 2011.

[6] G. Gazetas, E. Garini, and A. Zafeirakos, "Seismic analysis of tall anchored sheet-pile walls," *Soil Dynamics and Earthquake Engineering*, vol. 91, pp. 209–221, 2016.

[7] J. Leal, J. C. De La Llera, and G. Aldunate, "Seismic isolators in pile- supported wharves," *Proceedings of Ports*, in *Proceedings of 13th Triennial International*, Seattle, WA, USA, August 2013.

[8] A. Zekri, A. Ghalandarzadeh, P. Ghasemi, and M. Hossain Aminfar, "Experimental study of remediation measures of anchored sheet pile quay walls using soil compaction," *Ocean Engineering*, vol. 93, pp. 45–63, 2015.

[9] C. W. Yu, C. J. Lee, W. Y. Hung, and H.-T. Chen, "Application of Hilbert-Huang transform to characterize soil liquefaction and quay wall seismic responses modeled in centrifuge shaking-table tests," *Soil Dynamics and Earthquake Engineering*, vol. 30, no. 7, pp. 614–629, 2010.

[10] L. Y. Wang, S. K. Chen, and P. Gao, "Research on seismic internal forces of geogrids in reinforced soil retaining wall structures under earthquake actions," *Journal of Vibroengineering*, vol. 16, no. 4, pp. 2023–2034, 2014.

[11] L. Y. Wang, G. X. Chen, and S. Chen, "Experimental study on seismic response of geogrid reinforced rigid retaining walls with saturated backfill sand," *Geotextiles and Geomembranes*, vol. 43, no. 1, pp. 35–45, 2015.

[12] K. Miyashita and T. Nagao, "A fundamental study on the simple evaluation method of the seismic performance of sheet pile quay walls with vertical pile anchorage against Level-one earthquake ground motion," *Journal of Applied Mechanics*, vol. 10, pp. 601–611, 2007.

[13] M. Sato and K. Tabata, "Shaking table test of a large-size model on failure mechanism of sheet-pile quay wall and pile foundation due to lateral spreading," *Japanese Geotechnical Journal*, vol. 4, no. 4, pp. 259–271, 2009.

[14] P. Ruggeri, D. Segato, and G. Scar-pelli, "Sheet pile quay wall safety: investigation of posttensioned anchor failure- s," *Journal of Geotechnical and Geoenvironmental Engineering*, vol. 9, no. 139, pp. 1567–1574, 2013.

[15] B. H. Wang, Z. H. Wang, and X. Zuo, "Frequency equation of flexural vibrating cantilever beam considering the rotary inertial moment of an attached mass," *Mathematical Problems in Engineering*, vol. 2017, Article ID 1568019, 5 pages, 2017.

[16] F. Kalantary, H. MolaAbasi, M. Salahi, and M. Veiskarami, "Prediction of liquefaction induced lateral displacements using robust optimization model," *Scientia Iranica A*, vol. 20, no. 2, pp. 242–250, 2013.

[17] R. Motamed and I. Towhata, "Mitigation measures for pile groups behind quay walls subjected to lateral flow of liquefied soil: shake table model tests," *Soil Dynamics and Earthquake Engineering*, vol. 10, no. 30, pp. 1043–1060, 2010.

[18] L. Y. Wang, G. X. Chen, P. Gao, and S. K. Chen, "Pseudo-static calculation method of the seismic residual deformation of a geogrid reinforced soil retaining wall with a liquefied backfill," *Journal of Vibroengineering*, vol. 17, no. 2, pp. 827–840, 2015.

[19] B. Jiang, "Studies on soil arching effect and earth pressure for retaining structure," Doctoral thesis, Zhejiang University, Hangzhou, China, 2005.

[20] H. Matlock and L. C. Reese, "Generalized solutions for laterally loaded piles," *Journal of Soil Mechanics and Foundations Division*, vol. 86, no. SM5, pp. 63–91, 1960.

[21] A General Team Planning Group of the Third Design Institute of the Ministry of Railways, "Calculation of bridge pier foundation considering soil elastic resistance," *Railway Standard Design Newsletter*, no. 7, pp. 8–42, 1972.

[22] J. E. Bowles, *Analytical and Computer Methods in Foundation Engineering*, McGraw-Hill, New York, NY, USA, 1974.

[23] W. T. Fan, "Dimensionless coefficient of "K" method in single pile calculation," *Railway Standard Design Newsletter*, no. 2, pp. 38–45, 1975.
[24] Ministry of Communications of Road Planning and Design Institute, *Highway Bridges and Culvert Design Specifications (Trial)*, China Communications Press, Beijing, China, 1975.
[25] Y. H. Chen, "Discussion on calculation of earth pressure of high parallel wall," *China Rural Water Conservancy and Hydropower*, vol. 11, pp. 53-54, 2002.